energies

MDPI

Article

A Methodological Analysis Approach to Assess Solar Energy Potential at the Neighborhood Scale

Gabriele Lobaccaro [1,*], Malgorzata Maria Lisowska [1], Erika Saretta [2,3], Pierluigi Bonomo [2] and Francesco Frontini [2]

1 Department of Architecture and Technology, Norwegian University of Science and Technology, 7491 Trondheim, Norway
2 ISAAC-SUPSI, Campus Trevano, CH 6952 Canobbio, Switzerland
3 Department of Architecture, Built environment and Construction Engineering, Politecnico di Milano, 20133 Milano, Italy
* Correspondence: gabriele.lobaccaro@ntnu.no; Tel.: +47-918-13-568

Received: 11 August 2019; Accepted: 8 September 2019; Published: 17 September 2019

Abstract: Rapid and uncontrolled urbanization is continuously increasing buildings' energy consumption and greenhouse gas emissions into the atmosphere. In this scenario, solar energy integrated into the built environment can play an important role in optimizing the use of renewable energy sources on urban surfaces. Preliminary solar analyses to map the solar accessibility and solar potential of building surfaces (roofs and façades) should become a common practice among urban planners, architects, and public authorities. This paper presents an approach to support urban actors to assess solar energy potential at the neighborhood scale and to address the use of solar energy by considering overshadowing effects and solar inter-building reflections in accordance with urban morphology and building characteristics. The approach starts with urban analysis and solar irradiation analysis to elaborate solar mapping of façades and roofs. Data processing allows assessment of the solar potential of the whole case study neighborhood of Sluppen in Trondheim (Norway) by localizing the most radiated parts of buildings' surfaces. Reduction factors defined by a new method are used to estimate the final solar potential considering shadowing caused by the presence of buildings' architectural elements (e.g., glazed surfaces, balconies, external staircases, projections) and self-shading. Finally, rough estimation of solar energy generation is assessed by providing preliminary recommendations for solar photovoltaic (PV) systems suited to local conditions. Results show that depending on urban morphology and buildings' shapes, PV systems can cover more than 40% of the total buildings' energy needs in Trondheim.

Keywords: solar energy; solar potential mapping; solar neighborhood planning; BIPV; BAPV

1. Introduction

By 2050, 75% of the world's population is expected to live in cities because of a massive migration process from rural to urban areas [1–3]. This has contributed to the creation of more complex high density urban environments creating more challenges to the efficient deployment of Renewable Energy Sources (RES), especially for solar energy accessibility and related applications, such as solar system integration [4,5]. Today, solar systems are not only seen as a means for energy generation but they are increasingly conceived as an integrated architectural element, as architects have successfully demonstrated the potential of using solar modules as building materials with aesthetic functions, in addition to being active and profitable building skin elements.

The complexity of the built agglomerations (such as building volumes, urban or building typological factors, density, vegetation, etc.) often affects the incidence of solar irradiation on the buildings' surfaces

by creating non-optimal scenarios for solar systems (e.g., partial shading or localized hot spots causing overheating), which in turn leads to power losses, non-optimal operating conditions caused by potential malfunctions, or safety and reliability reduction effects. Moreover, the analysis of constraints at the urban scale allows determination of the solar potential of construction surfaces in a more realistic way, owing to the analysis of typological factors and a sensitivity analysis of their relation with solar technology exploitability by introducing weighting indicators to translate the different constructive, geometric, and typological constraints that affect the solar system's integration [6]. Thus, shading from surrounding buildings and solar inter-building reflections are becoming common issues in relation to the deployment of solar systems on façades and roofs in such highly densified urban environments. Therefore, preliminary solar potential and shading analysis are important to secure "right to light", solar accessibility, and to avoid common urban planning mistakes [5,7]. In fact, because architects and urban planners often do not have sufficient knowledge and time to assess the potential of solar energy during the design process, having a technical background and setting a proper time for analyses would not only lead to the solar energy harvesting potential being maximized, it would also mean they would be more likely to study more efficient design solutions for integrating solar systems on building envelopes [8]. Furthermore, municipalities should adopt support planning instruments to optimize the use of solar energy potential through orientation, angle, irradiation, and solar energy generation from solar systems architecturally integrated on roofs, façades, and other relevant locations (e.g., parking shelters). In this scenario, solar mapping of urban surfaces is shown as a promising approach worldwide [9–11]. However, the analysis of the most recent existing methodologies for solar maps in Europe (Section 2.1) allowed individualization of the existing research gaps to assess solar energy potential at the neighborhood scale.

This study presents an approach showing how some of the existing research gaps can be potentially overcome by considering overshadowing effects and solar inter-building reflections in accordance with urban morphology and building characteristics. The approach is applied on a case study located in Trondheim (Norway) (Section 2.2), where integrated design solutions to exploit solar energy potential are continuously increased (Section 2.3). The approach couples existing validated tools with new methods [e.g., Façade Active Solar TICINO (bFAST) [6,12]] in a logical sequence of six steps described in the methodology section (Section 3). Its application is presented (Section 4) and discussed (Section 5) in relation to local conditions. The paper closes with conclusions and outlooks for further work (Section 6).

2. Background and Motivation

2.1. State-Of-The-Art of the Existing Solar Mapping

Solar maps support the localization of the most suitable buildings' surfaces to predesign the solar system installations and they allow quantification of the potential of solar energy harvesting. Most cities have started to implement online solar maps, which provide information on solar energy potential and generation produced on the roofs of existing buildings, but there are also some examples that consider the solar potential of planned buildings [13]. This practice can guide the urban densification process while optimizing the exploitation of the solar energy potential on roofs and façades. Even though the literature review of solar maps recently developed in Europe is not exhaustive since the research should be done in the local language (Table 1), the majority of the analyzed solar maps are based on geometry data (i.e., buildings, terrain, vegetation) obtained through light detection and ranging (LiDAR) data. The 3D information is focused on irradiation analysis and energy generation by photovoltaic (PV) systems, though sometimes solar thermal (ST) output is also available [14]. One of the main research gaps associated with existing solar maps is that the majority of maps are available for the estimation of solar potential for small-scale roofing installations, not for integrated solar façade systems [15]. In some cases, categories to assess solar energy potential are not clearly defined, as in the case of solar maps for Vienna and Berlin.

Table 1. List of ten selected existing solar maps in Europe that have been recently developed.

Area	Nr	City/Country	Analyzed Building Envelope Elements	Solar System	Module Efficiency/Energy Output	Categories	Solar Irradiation Ranges (kWh/m^2/year)	Base for Categories
North Europe	1	Norway	Roofs	PV	PV: 16%/Yes	Unsuitable Suitable Very suitable	N/A	Solar irradiation, roof geometry
	2	Stockholm, Sweden	Roofs	PV/ST	PV: 14%/Yes ST: 50%/Yes	Hesitant Promising Excellent	<950 950–1000 >1000	Solar irradiation, roof geometry
	3	Copenhagen, Denmark	Roofs	N/A	N/A	Not good Reasonable Good Very good	N/A	Solar irradiation
Central Europe	4	Berlin, Germany	Roofs	PV	12%/Yes	Reasonable Good Very good	<920 920–1035 1035–1093	N/A
	5	Bristol, United Kingdom	Roofs	PV	N/A/Yes	Reasonable Good Very good	<950 950–1000 >1000	Solar irradiation
	6	Vienna, Austria	Roofs	PV/ST	PV: 14%/Yes ST: 90%/Yes	Good Very good	900 < 1200 >1200	Solar irradiation
	7	Switzerland	Roofs	PV/ST	PV: 17%/Yes (PV both for façades and roofs) ST: varies based on statistical data	Low Medium High Very high Excellent	<800 800–1000 1000–1200 1200–1400 >1400	Solar irradiation, roof geometry
			Façades			Low Medium High Very high Excellent	<600 600–800 800–1000 1000–1200 >1200	
	8	Genève, Switzerland		PV/ST	N/A	Favorable Very favorable	<1200 >1200	Solar irradiation, roof geometry
	9	Lyon, France	Roofs	PV	PV: 15.5%/Yes	Bad Low Average Very good Good Excellent	<350 350–650 650–850 850–1100 1100–1250 1250–1344	Solar irradiation, roof geometry
	10	Annecy, France	Roofs	PV	PV: 15.5%/Yes	Bad Fair Way Good Very good Excellent	<1093 1093–1166 1166–1238 1238–1311 1311–1384 >1384	Solar irradiation
	11	Bordeaux, France	Roofs	PV	N/A	Fair Good Excellent	1080–1230 1230–1390 1390–1540	Solar irradiation
South Europe	12	Bolzano	Roofs	PV	Cadmium telluride photovoltaics and poly crystalline silicon/Yes	NA	<800 800–1000 1000–1200 >1200	Solar irradiation, roof geometry
	13	Bologna, Italy	Roofs	PV/ST	N/A	Low Average Very good Good Excellent	<500 500–800 800–1100 1100–1400 >1400	Solar irradiation
	14	Lisbon, Portugal	Roofs	N/A	N/A	Class I Class II Class III Class IV	<1000 1000–1400 1400–1600 >1600	Direct solar irradiation, roof geometry
	15	Vitoria-Gasteiz, Portugal	Roofs	N/A	N/A	Class A Class B Class C Class D Class E Class F Class G	0–5% 5–10% 10–20% 20–30% 30–40% 40–50% >50%	Solar potential

PV: Photovoltaic; ST: Solar thermal; N/A: data not available.

Other gaps are related to the calculation methods. Studies show that the most common calculation methods are based on the "constant irradiation level" [16,17]. In the case of the solar map of Norway, the calculation is based on Photovoltaic Geographical Information System (PVGIS), a European solar mapping program that uses satellite data but does not consider overshadowing effects due

to the presence of other buildings. PVGIS also does not consider solar inter-building reflections [18], which are not taken into account in any of the other existing solar maps as well [17].

The solar map of Switzerland is an example of advanced solar maps. It allows visualization of values in an interactive 2D map, including values of solar irradiation on both roofs and façades of the buildings of the whole country, categorization of irradiation results, and availability of both PV and ST outputs and user-friendly visualization of the results [19]. The 3D information about the buildings comes from the dataset swissBUILDINGS^{3D} 2.0 [19,20]. Global irradiation data is derived from satellite data from MeteoSwiss and the temperature data is taken from ground measurement stations for the years 2004–2014 [20]. The Perez sky model is used for global irradiation data collection. Therefore, direct, diffuse irradiation and solar reflections from the ground are calculated in the middle point of each surface; shadowing due to the presence of nearby buildings and the vegetation elements is also taking into account, while solar inter-building reflections are not considered. Solar energy generation options with PV coverage of 25%, 50%, and 100% of the façade are presented. When it comes to the potential of the roofs, alternatives of 50%, 75%, and 100% of surface coverage with PV systems are available. According to the Swiss Federal Office of Energy, modules of efficiency of 17% and a performance ratio of 80% are used for solar energy generation calculations [19,20]. The efficiency of ST energy is based on a statistical data-dimensioned system. However, in the solar map of Switzerland, the calculations for solar energy generation are made without any distinction between windows and opaque walls, while any architectural elements or obstructions such as balconies or staircase that reduce the solar potential of surfaces are considered [6,20].

This latter aspect represents one of the major research gaps of the existing solar maps that the presented approach aims to overcome. In the solar energy potential calculations of both the roofs and the façades, this approach considers the solar reflections from other buildings and the ground, along with the shadows due to the presence of geographic elements (e.g., orography of the terrain) and other structures (e.g., fabrics).

Furthermore, a method [6] to estimate the real available area for PV system installation by considering architectural factors and buildings' physical elements (e.g., glazed surfaces, balconies, external staircases, projections) has been applied.

2.2. Solar Energy Potential in Norway

One of the challenges associated with solar energy in Norway is uneven annual distribution of solar irradiation. In Trondheim (latitude 63° N), the solar irradiation varies substantially from low values in winter to abundance of irradiation in summer, as well as variations caused by daylight availability and sun height. In summer, daylight hours are up to almost 21 h, while in winter they can be as shorts as 4 h and 30 min [21].

Regarding sun height, in Trondheim it is 50° in summer solstice, while in winter solstice it is only 5°. Because of low sun elevation in winter, harvesting solar energy through building integrated PV systems on the façades is a good alternative and such solutions are more often applied in Norway. In the office building Solsmaragden in Drammen, the façades were covered with integrated PV cells [22,23]. The Powerhouse in Trondheim was shaped to maximize solar energy harvesting potential and energy generation from PV systems [24,25] by placing cells on the roof, southern façade, and on top of the western façade of the building. This allows to reach the Zero Emission Building-Construction, Operation and production of building Materials (ZEB–COM) level, which balances the amount of energy produced by RES in the building with the greenhouse gas (GHG) emissions from construction, operation, and production of the buildings' materials [26].

These examples show the growth in solar power installations in Norway, which in 2016 registered 75% more installations compared to 2015, while data from 2018 shows a further increase of more than 4 times compared to 2015 [7,27]. Other challenges related to solar energy in Norway are associated with high cloud coverage, significant amounts of precipitation and snowfall, and long darkness periods [28], while low air temperature is both challenge and opportunity because it contributes to maintaining optimal efficiency of PV systems [29].

Another general issue is associated with urban density, even if Norwegian urban environments are mostly characterized by low–medium urban agglomeration. An example in that sense is a commercial building located in the Lerkendal district in Trondheim, where PV panels placed on the western and southern façades were shadowed by the presence of a new residential block built on the south side causing a significant reduction of solar energy potential [7]. This example demonstrates that tools such as solar maps, through preliminary solar accessibility and solar potential analyses, can prevent and avoid common urban planning mistakes that can lead to misplaced location of solar systems with consequent decrease in energy production.

2.3. Case study Area

The approach is applied in the case study area of Sluppen, located in the south of Trondheim. Currently, the Sluppen area is surrounded by the Nidelva river and it is dominated by industrial buildings and numerous parking areas, while residential buildings are located in the southeastern part. The E6 highway and Holtermanns veg, the main road for access to the city center from the south, separate the neighborhood and block access to greenery (Figure 1).

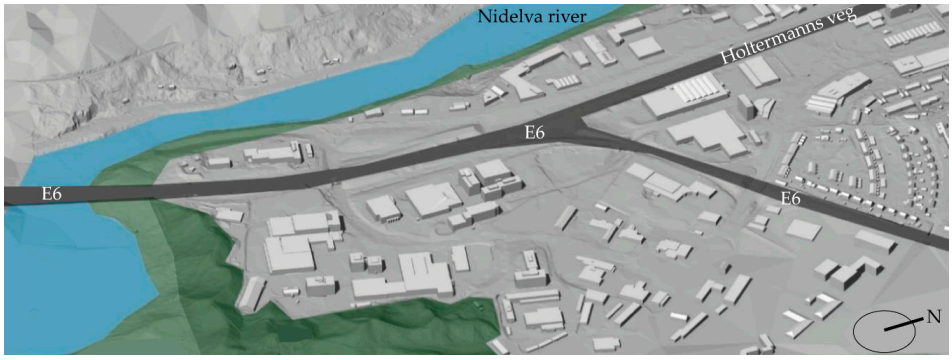

Figure 1. Overview of the Sluppen area.

According to the Norwegian planning guidelines, the municipalities should develop more compact cities to reduce the use of land and the GHG, and to promote environmentally friendly means of transport; attractive, livable, and enjoyable living areas; and the exploitation of RES [30,31].

In that regard, Sluppen has the ambition to become a car-free district by hosting mixed-use functions ranging from new technology firms to research and education centers, residential and service buildings, and urban public spaces [32]. Different design proposals (Figure 2) resulting from the Sluppen 2050 competition [33] were mostly focused on solving transport challenges associated with increased building density, while no design drivers were set for solar accessibility and solar potential.

Figure 2. New and existing buildings in the existing situation (**a**), feasibility studies I (**b**) and II (**c**).

3. Methodology

The methodological analysis approach consists of a logical sequence of six steps (Figure 3).

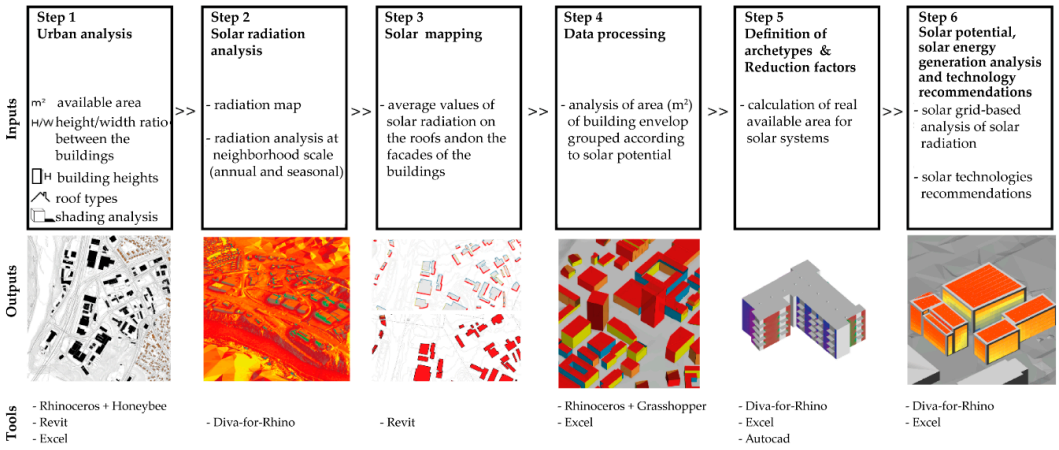

Figure 3. Workflow of the approach to assess solar energy potential at the neighborhood scale.

It is based on two complementary methodologies developed in Switzerland: the first one for mapping the solar potential of the existing building stock (both roofs and façades) [20], and the second one for detailing the potential of installation for Building Integrated Photovoltaic (BIPV) systems in urban areas of the Ticino Region [6,12].

The novelty of the proposed approach stands in coupling these methods in a logical and sequential chain of steps with simulation modelling, analysis, and processing tools that allow potential solutions to be proposed for the individualized research gaps in the existing solar maps.

3.1. Step 1–Urban Analysis

The first step aims to analyze the most important urban parameters influencing the solar potential. First, the number of buildings and their main orientation are described. Then, a series of analyses to evaluate the impact of urban characteristics on the solar potential are performed (Table 2).

Table 2. Types of analyses conducted in Step 1—Urban Analysis.

Type of Analysis	Description	Categories
Analysis of BRA *	Determines the building density in urban areas in Norway [34].	very low (0–5000 m^2) low (5000–10,000 m^2) medium (10,000–15,000 m^2) medium-high (15,000–20,000 m^2) high (20,000–25,000 m^2) very high (> 25,000 m^2)
Analysis of building heights	Analyzes the height of the building in the district area.	low (0 < H < 20 m), medium (20 < H < 40 m) high (H > 40 m).
Analysis of height/width	Takes into account the aspect ratio between heights (H) of the building and the distance (W) between them.	very low (0.0 < H/W < 2.0) low (2.0 < H/W < 4.0) medium (4.0 < H/W < 6.0) high (6.0 < H/W < 8.0) very high (H/W > 8.0)
Analysis of roof types	Analyzes the morphology of the roofs.	flat and pitched roofs
Analysis of shading	The analysis, run in Ladybug for Grasshopper, presents the seasonal variations of the buildings' shading.	solstices and equinoxes

* BRA: bruksareal (Norwegian); usable heated floor area (English).

The urban analysis starts by extracting all of the building information (e.g., heights of the buildings, available area) from the 3D model developed in Rhinoceros environment, while the database is developed

in Excel. The rest of the urban analysis is conducted in Revit. Information related to each building is addressed in different maps with analysis of urban characteristics.

3.2. Step 2–Solar Irradiation Analysis

This step performs the solar irradiation analysis at the district level in order to identify the solar potential of the roofs and façades. To estimate both direct and diffuse solar irradiation, as well as solar reflections from the ground and the surrounding buildings, the Radiance parameters are set for the simulation (Table 3) and for the materials (Table 4). Yearly and seasonal solar irradiation analyses are conducted through Diva-for-Rhino by using the 3D model of the analyzed area.

Table 3. Radiance parameters used in irradiation simulations.

ab	ad	as	ar	aa
0–3	1000	20	300	0.1

ab: Ambient bounces; ad: Ambient division; as: Ambient super-samples; ar: Ambient resolution; aa: Ambient accuracy.

Table 4. Radiance parameters for the materials used in the solar irradiation analysis.

Surface	R	G	B	SP	RG	Analysis Period (Start dd.mm–End dd.mm)
Façade	0.35	0.35	0.35	0.00	0.00	01.01–31.12
Roof	0.35	0.35	0.35	0.00	0.00	01.01–31.12
Ground (Asphalt)	0.20	0.20	0.20	0.00	0.00	21.03–20.12
Ground (snow)	0.90	0.90	0.90	0.00	0.00	21.12–20.03

The simulation period is annual for façades and roofs. The ground surface properties change during the year instead (asphalt in spring, summer, and autumn; snow in winter). SP: Specularity; RG: Roughness.

3.3. Step 3–Solar Mapping

In this step, a solar map is developed based on annual solar irradiation analyses (Step 2) in order to visualize the parts of the roofs and of the façades with the highest solar potential at the district level.

The solar map is partially based on the methods used for the solar map of Switzerland [19,20]. In order to identify the potential solar energy generation on the façades roofs, several aspects of the methodology developed for the Swiss solar map are adapted in the proposed approach. The same factors influencing solar irradiation are considered:

- Exposure of the urban surfaces (roofs, façades, and terrain) to solar irradiation;
- Orientation of the façades and roofs (flat and pitched);
- Shadows among the buildings and self-shading by other parts of the building, only when the protruding volume affects the middle point of the façade or roof surface;

The estimation of solar potential is obtained by conducting annual solar irradiation mapping through Diva-for-Rhino and collecting average values of solar irradiation in the middle point of each building's surface (Figure 4). Therefore, the parts of the façades and of the roofs partly shaded during the day or during some periods of the year are not considered in this stage. However, in the next steps a more detailed grid based analysis is conducted.

The obtained annual solar irradiation values are in the range of 0–1100 kWh/m^2, and this interval is divided into five categories: very low (0–220 kWh/m^{2}year), low (220–440 kWh/m^{2}year), medium (440–660 kWh/m^{2}year), high (660–880 kWh/m^{2}year), and very high (880–1100 kWh/m^{2}year). Then, annual solar irradiation values for each surface are imported into Revit and represented as 2D surfaces for the roofs and 2D lines for the façades. Different colors and line thicknesses for the façades have been assigned to indicate the solar potential, with the thickest lines in red and dark red representing high and very high solar potential, average line thickness in orange representing medium solar potential, and the thinnest lines in yellow and blue representing façades with very low and low solar potential.

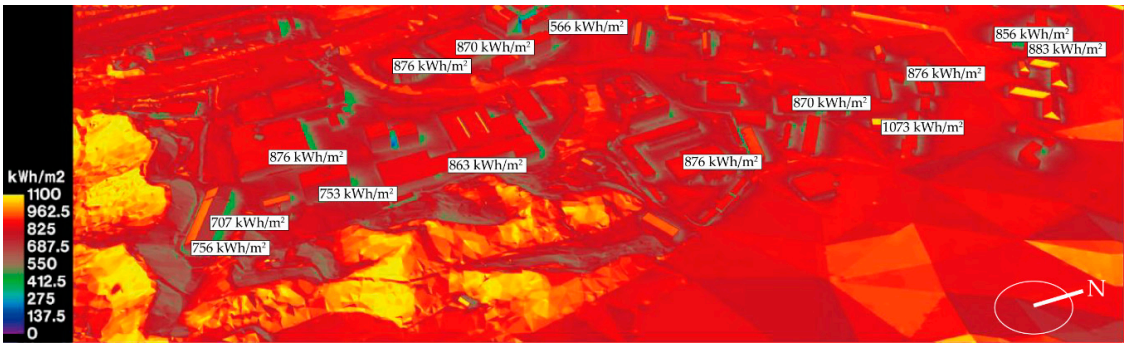

Figure 4. Annual irradiation map of Sluppen. The labels show irradiation values at selected points.

3.4. Step 4–Data Processing

At this stage, the outputs of the urban analysis (Step 1) are linked with the solar mapping elaborated in Revit (Step 3) to investigate how the urban morphology influences the solar potential at the district level. After the elaboration of solar maps for roofs and façades (Step 3), the 3D model is transferred into the Grasshopper environment and is used as a visual to identify the solar potential for the entire analyzed district, using different colors depending on the average value of solar irradiation impinging on the surfaces.

Furthermore, the other aspects of the urban analysis, such as the map related to the aspect ratio between the height (H) of the building and width (W) of the street, H/W (i.e., urban density), are combined with the solar potential of the whole district to visually show their relation. Bar and pie charts elaborated in Excel show the solar potential of façades and roofs according to selected parameters (Table 5).

Table 5. Type of analysis included in the data processing.

Type of Analysis	Analyzed Surfaces	Analyzed Parameters	Outcomes
Surface area calculations	Roofs and façades	Orientation	Orientation of the roofs and façades of the buildings in the whole district
		Solar potential	Solar potential of the whole district
	Façades	Orientation, H/W ratio, solar potential	Influence of the H/W ratio and orientation on solar potential
		Orientation of the façades, height of the building, solar potential of the façades	Influence of the height of the buildings and orientation of the façades on solar potential

3.5. Step 5–Definition of Building Archetypes and Reduction Factors

This step of the approach aims to define the architypes and to assess the effective available area for PV system installation on façades and roofs by considering architectural elements, obstructions, and glazed surfaces. In fact, the total surface of the building's envelope is usually strongly reduced by the shadings of architectural elements and obstructions (i.e., balconies and external staircases), as well as by the presence of the glazed surfaces (windows), which can only be partially replaced with PV systems.

The calculation of the effective available area is performed by defining reduction factors that are grounded on an existing methodology developed to assess the solar potential of façades in the Swiss context of the Ticino region [6]. This methodology allows consideration of transparent and opaque building elements and typological obstructions such as balconies, chimneys, and eaves in order to assess the installation of PV systems on façades. The reduction factors (IR) are applied to the total gross façade area (S_{gr}), as shown in Equation (1). They were determined in accordance with the local urban and building features (Table 6).

Table 6. Description and calculations of the reduction factors.

Indicator	Aspects Considered by Indicator	Equation
IR_1	Presence of windows.	$IR_1 = \frac{S_{gr} - 0.8 \cdot S_{open}}{S_{gr}}$
IR_2	Presence of balconies.	$IR_2 = \frac{S_{acc}}{S_t}$
IR_3	Shading of balconies.	$IR_3 = \frac{\text{Area with irradiation value} > 440\ kWh/m^2y}{S_{gr}}$
IR_4	Self-shading by other elements of the buildings.	$IR_4 = \frac{\text{Area with irradiation value} > 440\ kWh/m^2y}{S_{gr}}$
IR_5	Presence of external elements of the building, for example, staircases.	$IR_5 = \frac{S_{gr} - S_{external}}{S_{gr}}$

S_{gr} is the gross façade surface (m^2), S_{open} is the windows surface (m^2), S_{acc} is the parapet surface (m^2), S_t is gross façade surface with balconies (m^2), and $S_{external}$ is external element surface (m^2).

The threshold irradiation value for IR_4 and IR_5 is set equal to 440 kWh/m^2year, because it represents the lowest threshold of the range of medium solar potential introduced in Step 3. Direct, diffuse, and reflected irradiation from the ground and other buildings are considered in their calculation. Different building typologies (Figure 5) located in Trondheim (Figure 6), defined as archetypes, are first analyzed in AutoCAD to assess which surfaces can be effectively used for BIPV or building applied photovoltaic (BAPV) systems (i.e., usable area for solar system installation).

$$S_{BIPV}\left(m^2\right) = S_{gr}\left(m^2\right) \times IR_1 \times IR_2 \times IR_3 \times IR_4 \times IR_5 \quad (1)$$

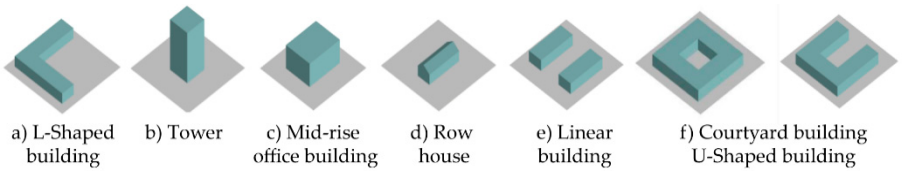

Figure 5. The most common types of building typologies analyzed in Trondheim.

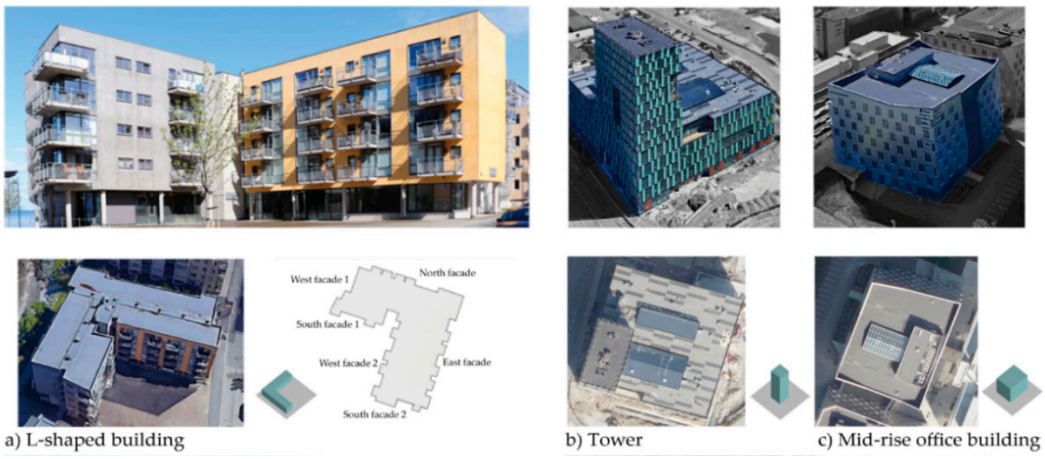

Figure 6. *Cont.*

Figure 6. Examples of the most common types of building typologies in Trondheim.

The archetypes were chosen by matching the building volumes designed in the feasibility studies with the criteria summarized in Table 7.

Table 7. Criteria for choosing buildings for reduction factor analysis.

Importance	Category	Criteria	Explanation
Primary	Year of construction	2000 or later	Majority of buildings in Sluppen are new, therefore buildings of no more than 20 years old are taken into consideration.
Secondary	Location	1. Proximity to or location within case study area. 2. Different building typologies located within one district.	Design of new buildings can be inspired by structures in new neighborhoods. Ilsvika district in Trondheim is chosen due to the presence of various building typologies (U-shaped buildings, L-shaped buildings, linear and row houses).

Calculation and Application of the Reduction Factors

The reduction factors are calculated and applied for all façades of the building typologies. Examples of the calculation of the reduction factors caused by the presence of windows (IR_1) and balconies (IR_2) are shown in Figure 7, where the unusable surfaces for solar systems are represented as grey areas, whereas the remaining opaque parts are assumed to be exploitable with crystalline silicon (c-Si) PV opaque claddings. Regarding the influence of transparent surfaces (considered through IR_1), only 20% of the opening's area is considered suitable for semi-transparent PV cladding. This setting was set in order to guaranteeing the penetration of light, especially in the winter period when sunlight is limited and the angle of the sun is very low. In fact, higher density of solar cells can reduce the availability of natural light in the indoor spaces. In the calculations of IR_2, it is assumed that the front parapet surface of the balconies can be used for installation of opaque solar installation, while the gross façade area behind the balconies is unsuitable for PV installation due to the self-shading. This factor also considers windows and doors placed between balconies. Solar irradiation analyses are conducted on each façade for IR_3, which relates to the reduction of solar potential due to the shading of balconies, and IR_4, which relates to reduction due to self-shading by other elements and projections of the buildings. Figure 8 shows an example for the south façades of an L-shaped building. Similarly, the reduction factor IR_5 is calculated considering the presence of external obstructions on the building, such as external staircases. In Table 8 the reduction factors for the L-shaped building are presented.

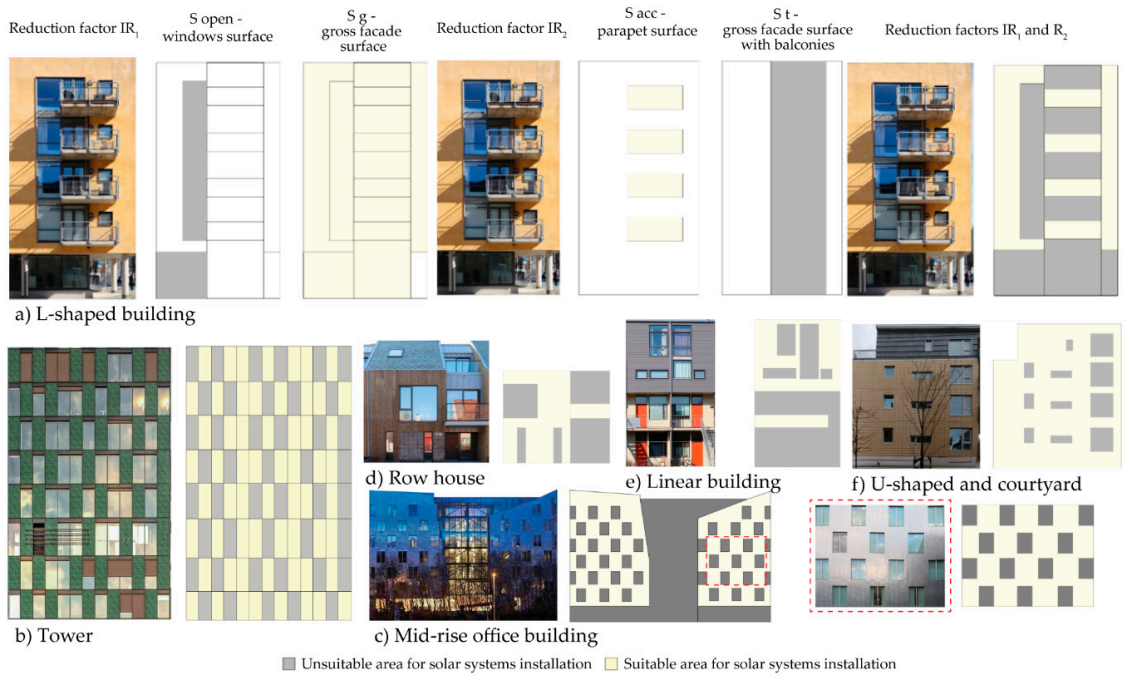

Figure 7. Examples of graphical calculation of the reduction factors IR_1 and IR_2 for the L-shaped building and a summary of the calculation of the factors for all of the building morphologies.

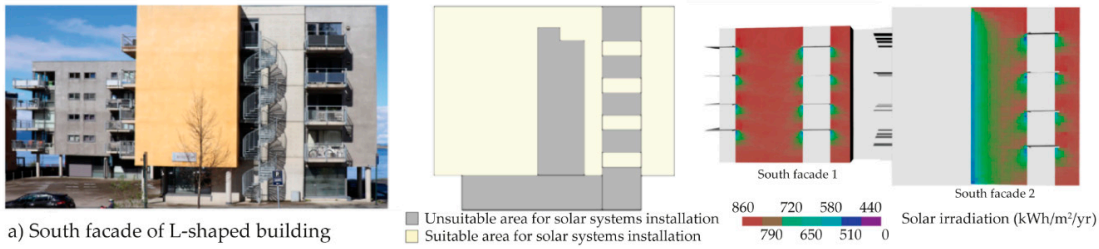

Figure 8. Examples of calculation of IR_3 and IR_4 for the south façades of the L-shaped building.

Table 8. Reduction factors for the façades of the L-shaped building.

Façade	S_{gr} (m^2)	IR_1	IR_2	IR_3	IR_4	IR_5	Total	S_{BIPV} (m^2)
Façade West 1	264	81%	70%	71%	64%	-	26%	68
Façade West 2	440	80%	60%	-	84%	73%	30%	132
Façade South 1	277	85%	71%	-	100%	76%	46%	127
Façade South 2	267	67%	37%	-	100%	-	25%	66
Façade North	612	81%	70%	-	-	-	54%	328
Façade East	640	88%	62%	51%	-	98%	27%	174
Average	2500	80%	62%	61%	87%	83%	22%	537

S_{gr}: total gross façade area; S_{BIPV}: usable area for solar system installation.

The same approach is used for the calculation of the reduction factors related to all of the façades of the different building typologies (Table 9). Regarding the roofs, the reduction factor IR_r is assumed equal to 25% due to the presence of chimneys, technical installations, etc. This value is based on scientific studies in literature, which show that a quarter of the total roof area is dedicated to maintenance service machines of the building, building installations such as antennas or plants, and other functions such as swimming pools, storage rooms, etc. [35,36].

Table 9. Calculated reduction factors for the analyzed building morphologies considering all of the surfaces (roofs and façades) of the building envelope.

Building Type	Building Morphology	IR_1	IR_2	IR_3	IR_4	IR_5	Total
Residential	L-shaped building	80%	62%	61%	89%	80%	22%
	Row house	56%	83%	-	-	-	47%
	U-shaped building	77%	64%	-	94%	-	46%
	Linear building	83%	77%	-	-	83%	53%
Office	Mid-rise	52%	-	-	-	-	52%
	High rise	47%	-	-	-	-	47%

3.6. Step 6–Solar Potential, Solar Energy Generation Analysis, and Technology Recommendations

In the final step, critical areas of the district characterized by high and low solar potential are identified based on the solar map (Step 3) and data processing (Step 4).

The analysis is performed to localize the best area of the building envelope to install PV systems and to evaluate their energy generation. Moreover, reduction factors (Step 5) are applied to all of the building typologies to make the solar energy generation analyses more accurate. These are performed on a group of buildings by conducting grid-based irradiation map analyses in Diva-for-Rhino. These analyses allow calculation of direct, diffuse irradiation and the contribution of solar inter-building and ground reflections.

In that regard, it is possible to identify the areas with the highest and the lowest solar potential. Parameters and material settings for the simulations are presented in Table 10 and in Table 4, respectively.

Table 10. Parameters used for grid-based irradiation simulations.

Solar Irradiation Component	Grid Size	ab	Metric	Outcomes
Direct irradiation	2 m × 2 m	0	Dayism-based hourly method	Produces an hourly result file (.ill) and time-cumulative irradiation rendering
Direct, diffuse irradiation and solar inter-building and ground reflections	2 m × 2 m	3	Cumulative sky method	Creates a cumulative sky Radiance distribution

The energy yield of a PV system is assessed using the following equation [37]:

$$\text{FinalYield} = \text{G}\left[\frac{\text{kWh}}{\text{m}^2\text{y}}\right] \times \text{Area}\left[\text{m}^2\right] \times \text{eff}[\%] \times \text{PR}[\%] \quad (2)$$

where G is the average value of solar irradiation on surface area, Area is the area of façade or roof (m^2), eff indicates the efficiency of the PV module (%), and PR stands for performance ratio.

Some assumptions are made for the calculation: the efficiency of PV modules is set equal to 22%, 17%, and 16% for roof modules, BIPV façade modules, and PV glass-to-glass modules (windows), respectively; the PR is set at up to 80%. The energy generation are calculated in order to evaluate how much of the total energy demand of the buildings can be covered by solar energy generation. Analyzed office and residential buildings are assumed to belong to the energy class A following Norwegian building regulations (NRB) [34]. A preliminary calculation of the total energy demand of the group of buildings and of the entire district is based on a simple calculation, where the value of the delivered energy per heated floor area of a building (Table 11) is multiplied for the number of buildings in the area. The buildings are assumed to belong to the class A according to the NRB.

Table 11. Delivered energy per heated floor area for different building categories.

Building Category	Delivered Energy per Heated Floor Area (BRA) (kWh/m^2)						
	Class A	Class B	Class C	Class D	Class E	Class F	Class G
Row houses	95 + 800/A	120 + 1600/A	145 + 2500/A	175 + 4100/A	205 + 5800/A	250 + 8000/A	>F
Apartment in block	85 + 600/A	95 + 1000/A	110 + 1500/A	135 + 2200/A	160 + 3000/A	200 + 4000/A	>F
Kindergarten	85	115	145	180	220	275	>F
Office	90	115	145	180	220	275	>F
School	75	105	135	175	220	280	>F
University	90	125	160	200	240	300	>F
Hospital	175	240	305	360	415	505	>F
Hotel	140	190	240	290	340	415	>F
Sport facility	125	165	205	275	345	440	>F

A: Part of the heated area of the total BRA [m^2].

Finally, recommendations for the most suitable and efficient PV system are given depending on the solar irradiation impinging on the building's surfaces. The technology is chosen considering the local conditions, such as orientation, exposure of roofs and façades, shadowing effect, and sensitivity to diffuse and reflected irradiation.

For façades, different products and systems are available on the market with high customizability and full integration with building skin technologies, such as cold façades, curtain walls, and double skin façades [38]. Those active claddings have the same appearance and functionality as other façade materials and ensure both constructive and architectural integration. The use of glass–glass active claddings containing c-Si solar cells is a reliable and market-ready option both for large glazing parts and for opaque parts, as they can be semi-transparent [39]. Glass–glass PV can also be a solution for windows due to their capacity to shade the inner space by producing energy, and at the same time maintaining an adequate level of natural light.

However, another technology that fits for building skin surfaces is thin film PV cladding. It can be opaque, semitransparent, and lightweight in some applications. Thin film PV cladding also works well in low and scattered light, and can harvest solar energy even in shaded areas.

4. Application in the Case Study Are of Sluppen

4.1. Step 1–Urban Analysis

Currently, the Sluppen area consists of 89 buildings and is characterized a by lack of organized urban planning. There are no dominant orientations of the buildings and the area is characterized by low building density. Buildings with very low BRA (BRA < 5000 m^2) dominate the area, with 76% of the fabrics (Figure 9a). In 93% of the area there are very low buildings (H < 20 m), while 7% of the structures are between 20–40 m of height (Figure 9b). The H/W aspect ratio is smaller than 2.0 in 90% of the buildings, while medium H/W is assumed for recently built buildings (Figure 9c). Only 8% of the buildings have pitched roofs, with the incidence angle varying between 20° and 35°.

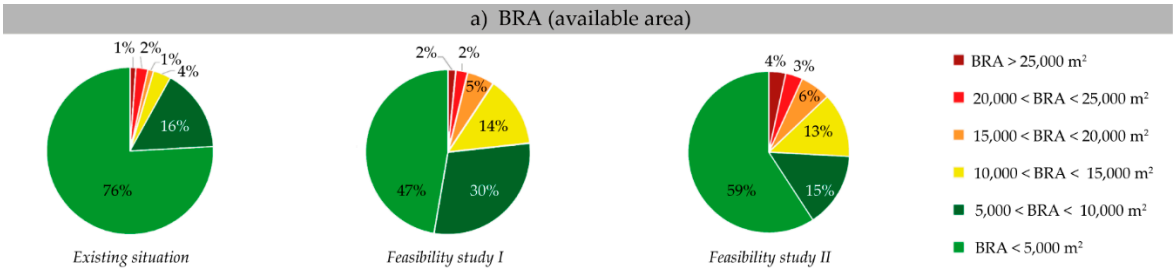

Figure 9. *Cont.*

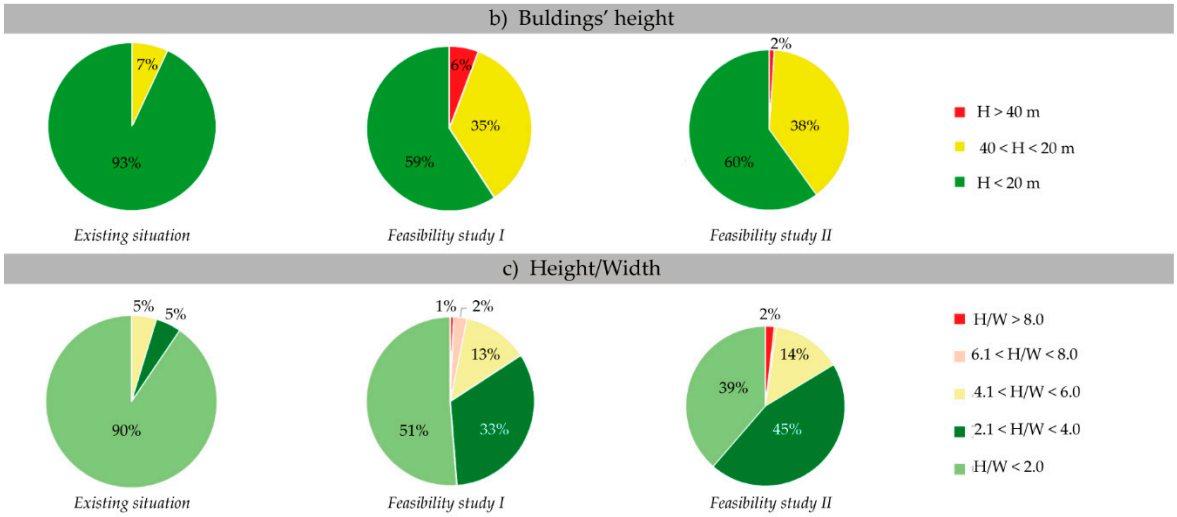

Figure 9. Urban analysis of Sluppen area: (**a**) BRA (m^2); (**b**) building height (m); (**c**) H/W analysis.

Feasibility study I consists of 131 buildings with two dominating orientations: NE-SW and NW-SE. Despite very low and low (5000 < BRA < 10,000 m^2) BRA dominating the area, covering for 47% and 30% of the dwellings, respectively, the %BRA for feasibility study I is more than 2.5 times greater than the existing situation (Figure 9a). Here, 59% and the 35% of the buildings have very low and low (20 < H < 40 m) heights, respectively (Figure 9b); for half of the buildings (51%) the H/W ratio is very low (H/W < 2.0) (Figure 9c); and 77% of the buildings have flat roofs, while 23% of the structures have pitched roofs with inclination angles varying from 15° to 40°.

Feasibility study II consists of 146 buildings and presents the same dominating orientations as in feasibility study I. The total %BRA is 3 times greater compared than in the existing situation, with 59% of total number of structures having low BRA (Figure 9a). The lowest buildings (59%) are situated in the peripheries of the neighborhood, while medium-height structures (39%) are located mainly between peripheries and the central part.

Two high-rise buildings (H > 40 m) are situated in the core of the district (Figure 9b), which is dominated by very low (39%) and low (45%) H/W ratio (Figure 9c). Buildings with flat roofs cover 87% of the area, while the remaining 13% of the structures have pitched roofs with low roof inclinations of around 20°.

4.2. Step 2—Solar Irradiation Analysis

Solar irradiation map analysis (Figure 10 shows an example related to feasibility study I) shows that in both existing and feasibility studies, the highest irradiation values are reached on the roofs in spring, while the lowest are reached in autumn (Table 12). In autumn and in winter, the highest values of solar irradiation are registered on the façades.

Table 12. Seasonal irradiation analyses in the existing situation and in the feasibility studies.

Analysis Period (Start dd.mm–End dd.mm)/Season	Average Solar Irradiation (kWh/m^2year)			Surfaces of the Building Envelope with Highest Solar Potential		
	Existing	Feasibility Study I	Feasibility Study II	Existing	Feasibility Study I	Feasibility Study II
21.03–20.06/spring	384	385	347	roofs	roofs	roofs
21.06–20.09/summer	347	347	333	roofs	roofs	roofs
21.09–20.12/autumn	58	58	62	façades	façades	façades
21.12–20.03/winter	58	66	70	façades	façades	façades

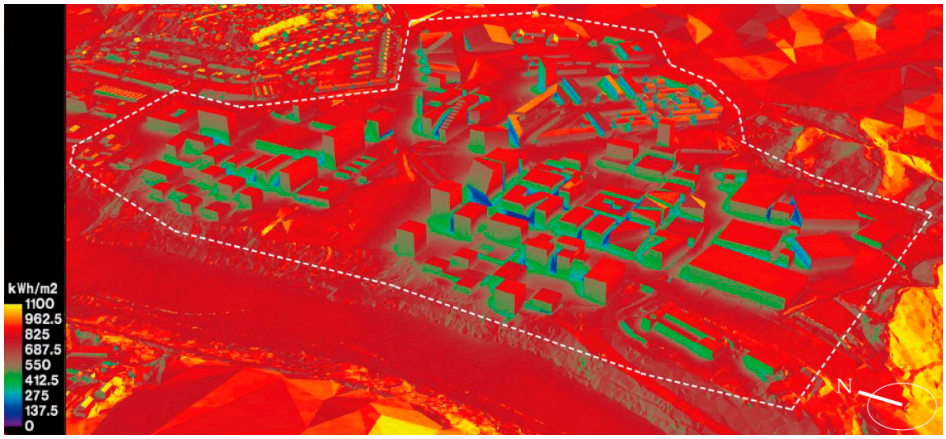

Figure 10. Example of the annual irradiation analysis for feasibility study I.

4.3. Step 3 and Step 4—Solar Mapping and Data Processing

The annual solar potential analysis on roofs and façades (Figure 11) shows that all the roofs' surfaces have high or very high solar potential and none of the surfaces has lower than medium solar potential in all of the analyzed scenarios. The solar maps show that around half of the façades in the existing situation range from high to medium solar potential because of the low building density and low H/W ratio, whereas in both feasibility studies around 30% of all of the façades register a similar solar potential.

Figure 11. *Cont.*

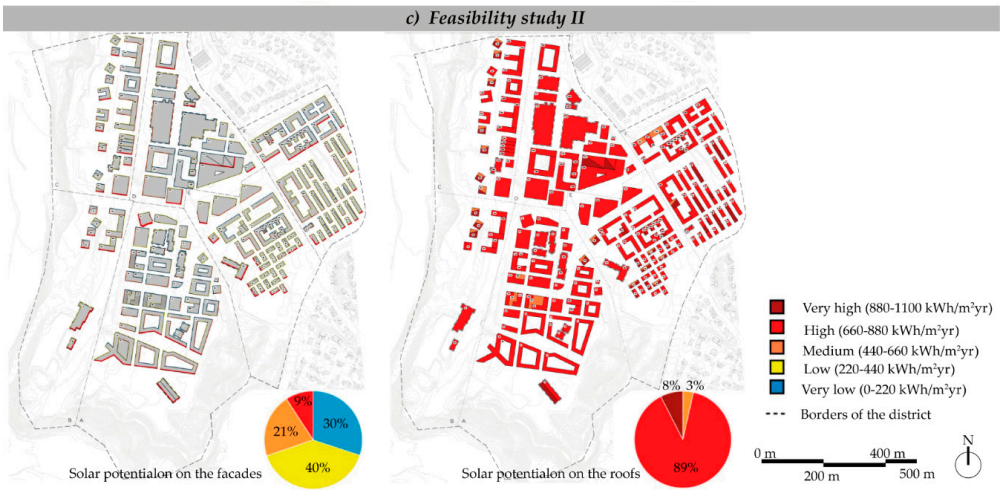

Figure 11. Solar map of the façades and roofs for the existing situation and the two feasibility studies.

In the existing situation (Figure 12), three-quarters of the façades and the roofs have high (73%) solar energy generation capability and 2% show very high solar potential. The majority of the roofs (94%) show high solar potential, and the remaining roofs have higher solar potential. On the other hand, only 35% of the façades have high solar potential, while 40% of them show very low solar potential, such as the area with new buildings. In this case, the H/W ratio ranges between 4.1 and 6.0 (Figure 13a) and the building height ranges between 20 m and 40 m.

In feasibility study I (Figure 14), all roofs range from medium to very high solar potential—88% have high solar energy potential, while 4% and 8% of them are characterized by medium and very high solar potential, respectively. Regarding the façades, 15% have high potential and there are no façades with very high solar potential because of the high density of the area (H/W > 8.0) (Figure 13b). More than one-third (32%) of the buildings higher than 40 m have high solar potential, while for buildings that are lower than 20 m, this percentage drops down to 15%.

In feasibility study II (Figure 15), 89% of the roofs are characterized by high solar potential, 3% have medium solar potential, and the remaining 8% show very high solar potential.

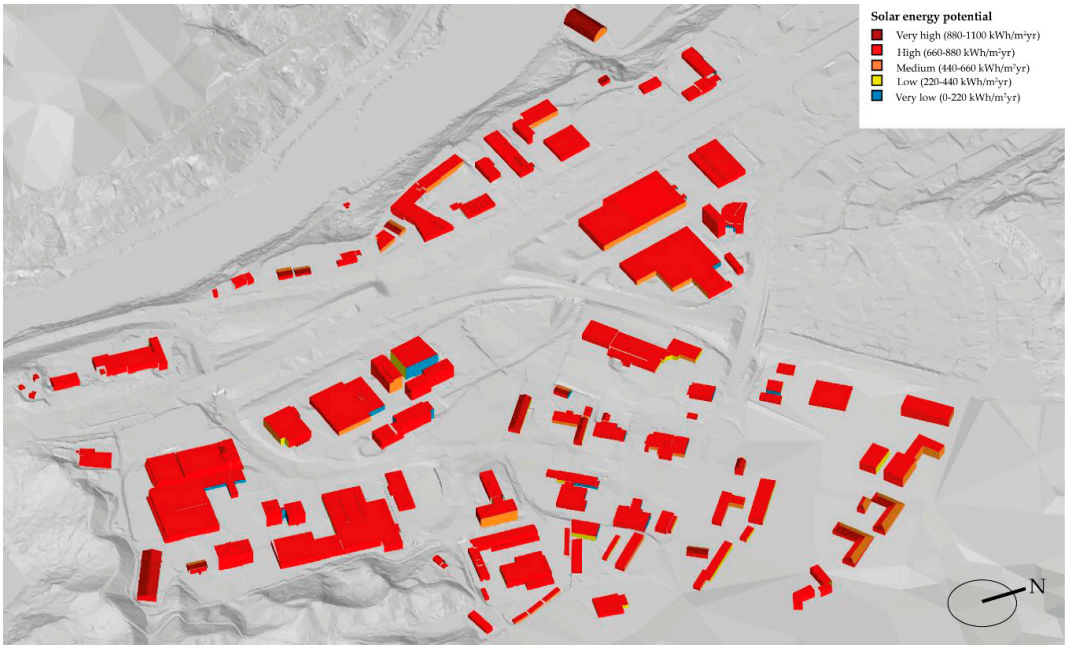

Figure 12. Three-dimensional visualization of the solar map for the existing situation.

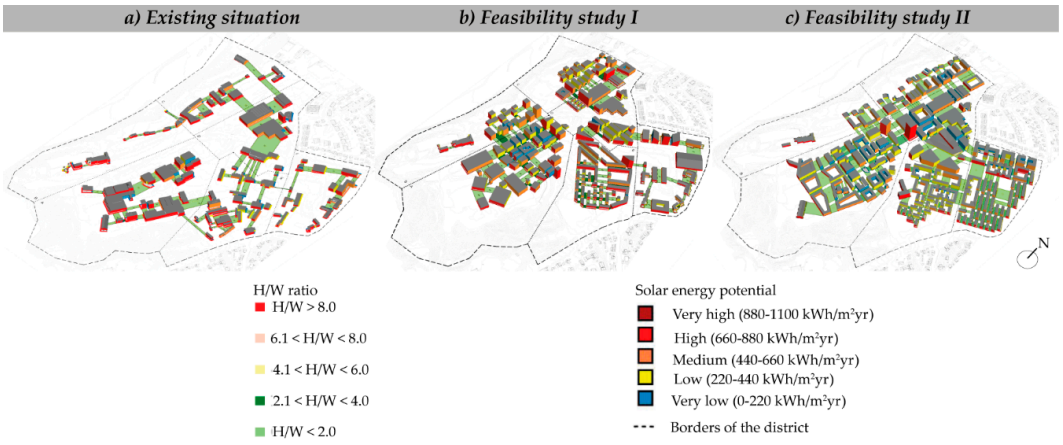

Figure 13. Solar potential of the façades depending on H/W ratio in the (**a**) existing situation, (**b**) feasibility study I, and (**c**) feasibility study II.

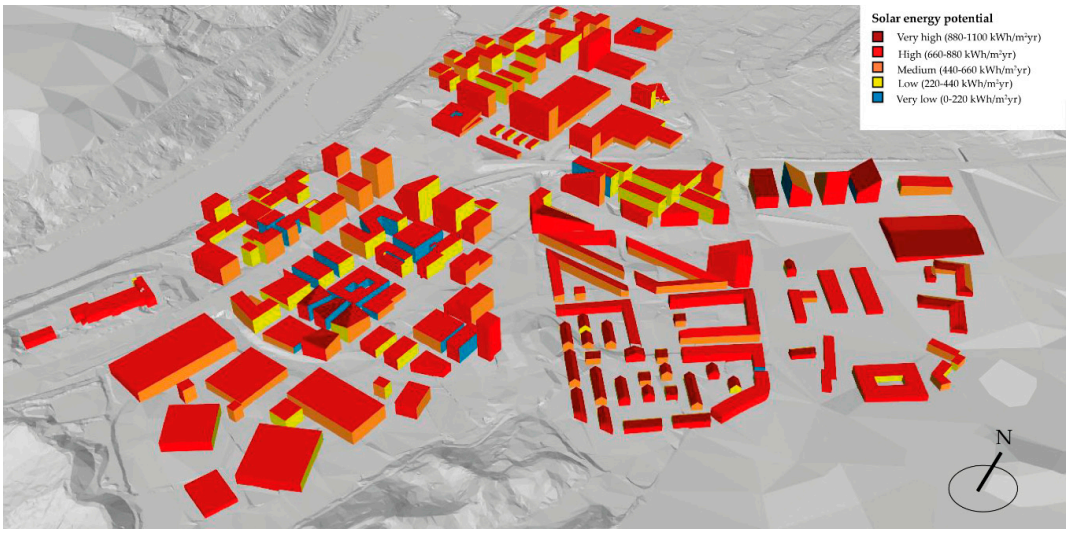

Figure 14. Three-dimensional visualization of the solar map for feasibility study I.

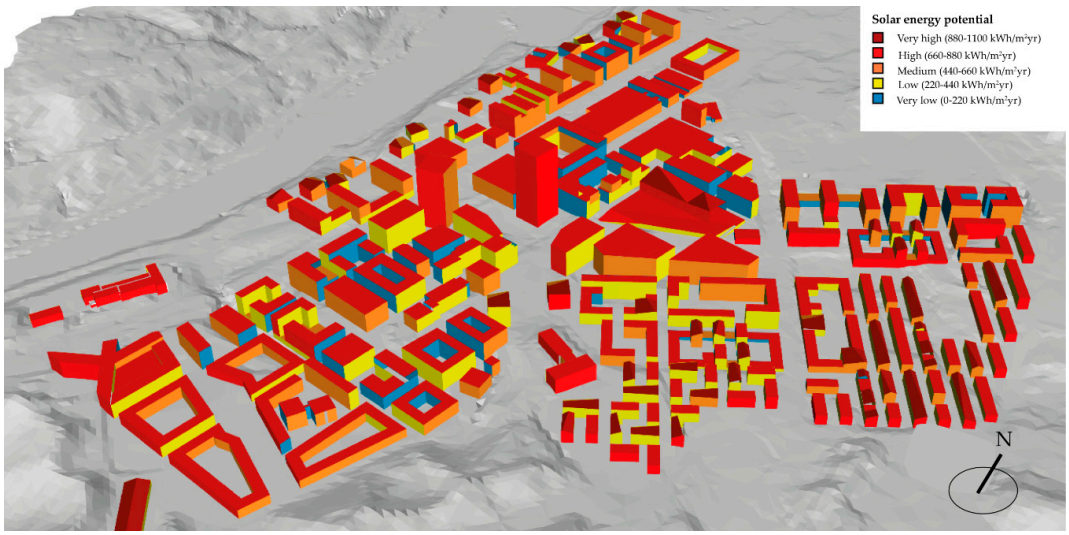

Figure 15. Three-dimensional visualization of the solar map for feasibility study II.

In total, 30% of the façades shows very low solar potential, followed by 40% with low potential, 21% with medium solar potential, while 9% show high potential (half of this group belongs to the buildings higher than 40 m (Figure 13c)). No façades show very high solar potential.

4.4. Step 5 and Step 6—Reduction Factor Application and Solar Potential, Energy Generation Analysis, and Technology Recommendations in Critical Areas

In this part of the approach, the reduction factors (Step 5) and the solar potential and energy generation analysis (Step 6) are applied on the buildings located in the three critical areas of the existing situation, feasibility study I, and feasibility study II.

The critical area (4700 m^2) in the existing situation is characterized by highest building density, where new buildings such as Stålgården Nord (Building 17), Sør (Building 16), and Rektangular (Building 18) have recently been added to the existing area (Figure 16). The grid-based solar analysis shows that 55% of the global solar irradiation is diffuse solar irradiation, while the remaining 45% is direct irradiation and solar irradiation from inter-building and ground reflections.

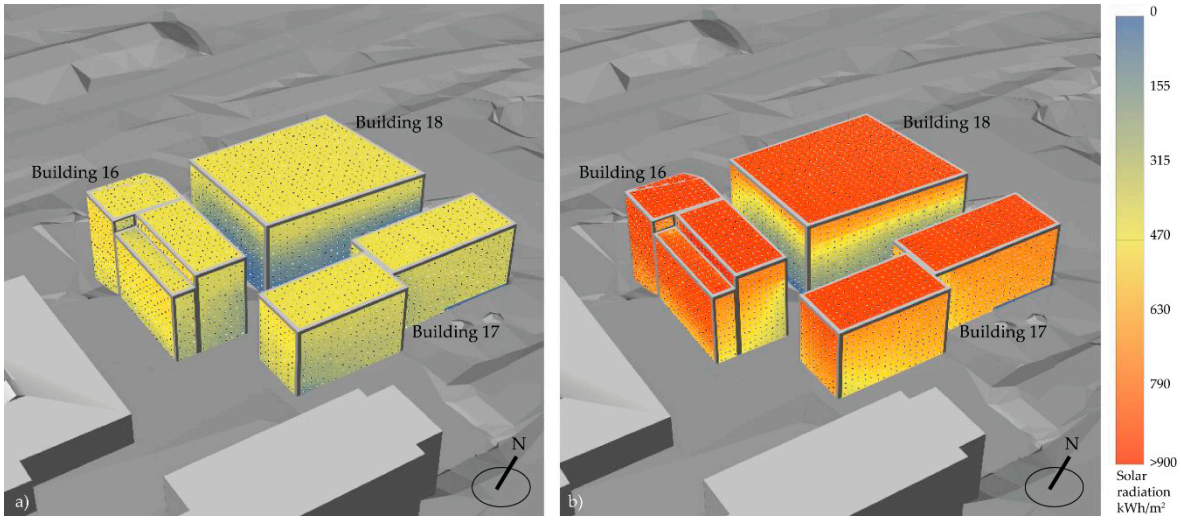

Figure 16. Annual analysis of direct solar irradiation (**a**) and global irradiation analysis (**b**) in the critical area in the existing situation.

On the roofs, the distribution of direct, diffuse irradiation and reflection is equally divided, while in the case of the façades, more than 65% is attributed to diffuse irradiation and solar reflections, and the rest (about 30%) is attributed to direct irradiation (Figures 16 and 17).

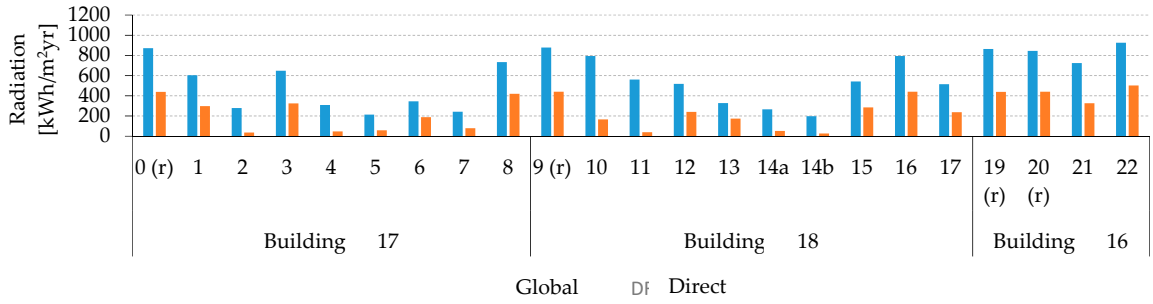

Figure 17. Average irradiation on the roofs (r) and façades in the critical area in the existing situation.

The outcomes underline that only for Building 16 is the average global solar irradiation on the façade (surface 22) higher than for the roof surfaces. For the solar energy generation calculation (Figure 18), reduction factors of 52% for the façades and 75% for the roofs are considered.

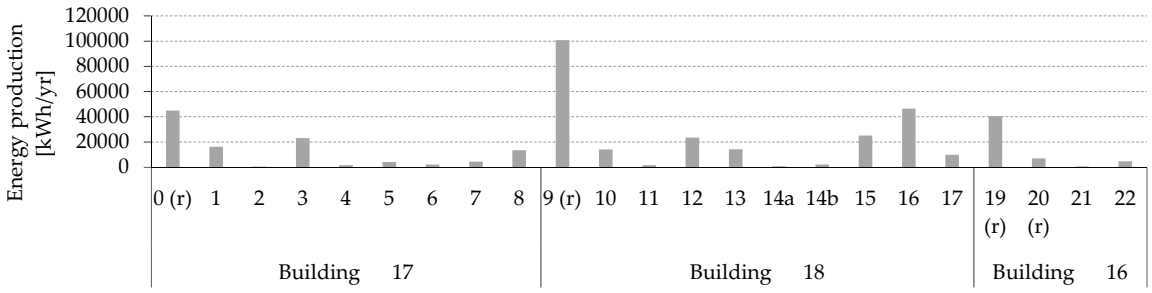

Figure 18. Solar energy generation on roofs (r) and façades in the critical area for the existing situation.

Generally, the outcomes underline that all of the buildings' surfaces are strongly affected by overshadowing effect. Regarding the solar energy generation analysis, the roof of Building 18 shows highest potential, followed by the façade of Building 16. Therefore, highly efficient monocrystalline technology is recommended for roofs, while for the façades thin film is recommended, given that this technology has reduced sensitivity to temperature and shading [40]. For the transparent surfaces, glass–glass PV modules can be used due to their two-fold capability to simultaneously produce energy and shade the inner space (Figure 19).

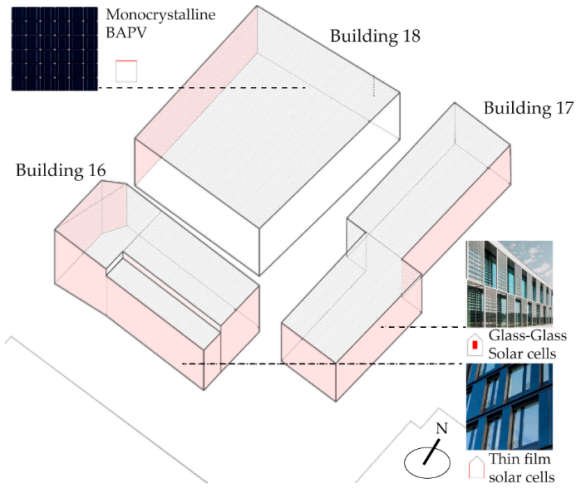

Figure 19. Solar technology recommendations for the critical area for the existing situation.

In feasibility study I, the critical area (2750 m^2) chosen for detailed solar irradiation analysis and solar energy generation is of high density, characterized by buildings of 20–40 m height and medium H/W ratio, which limits the solar accessibility on the street level. In this area, 52% of the total solar irradiation is diffuse and reflected from the ground and the buildings, while 48% is direct irradiation. This distribution holds true for roofs, while when façades are considered, almost two-thirds (65%) are of the total solar irradiation is from diffuse irradiation and solar inter-building reflections, while 35% is from direct irradiation (Figures 20 and 21).

The analysis in the critical area shows that the highest energy generation is from façades oriented southwest (Building 2 and Building 7), which are mainly unshaded by other buildings, while the pitched roof on Building 15b oriented southwest has the highest solar energy production, reaching 21,800 kWh/year.

Among façades, Building 13, oriented southeast, has the best solar potential, with an estimated production of around 15,000 kWh/year (Figure 22). Also, in feasibility study I the reduction factors of 52% for the façades and 75% for the roofs are used.

Regarding technology recommendations (Figure 23), an in-roof PV system is suitable for pitched roofs of every orientation, while BIPV systems can cover three of the façades that have the highest solar potential of the analyzed buildings.

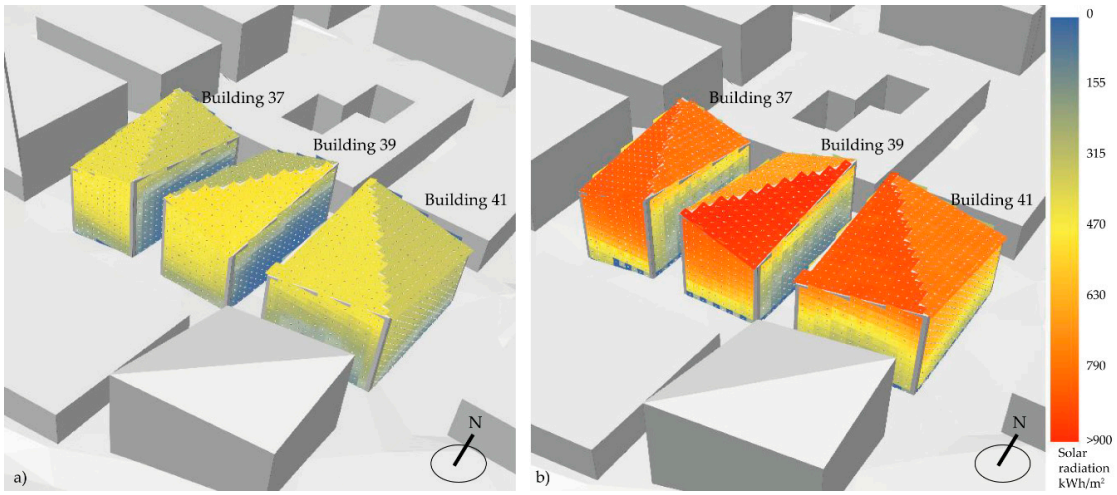

Figure 20. Annual analysis of direct solar irradiation (**a**) and global irradiation (**b**) in the critical area for feasibility study I.

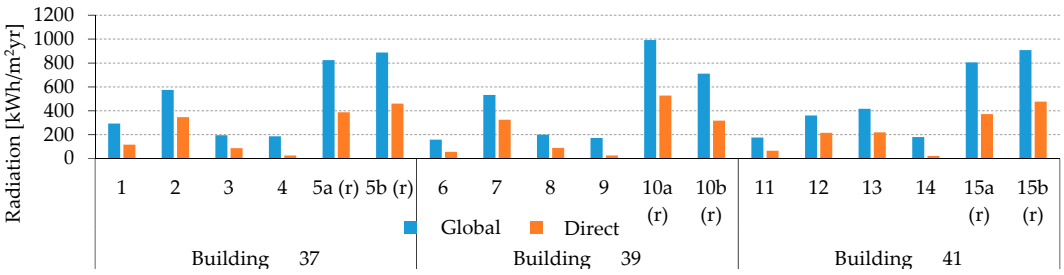

Figure 21. Average irradiation on the roofs (r) and façades in the critical area for feasibility study I.

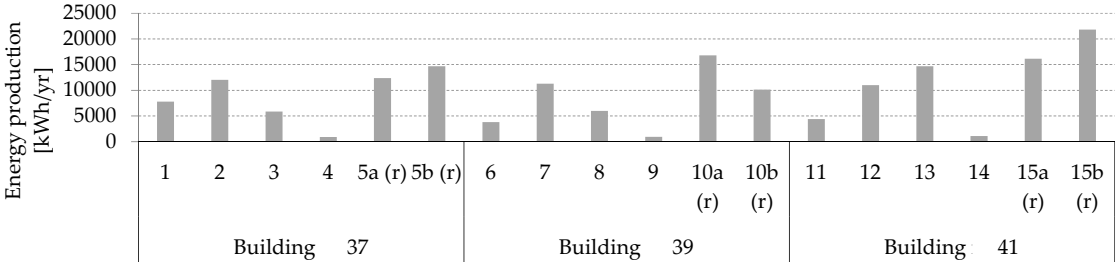

Figure 22. Solar energy generation on roofs (r) and façades in the critical area for feasibility study I.

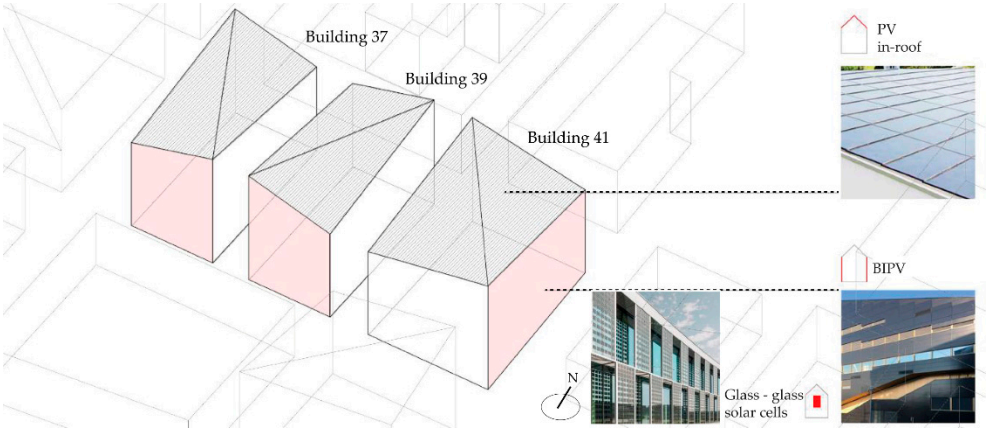

Figure 23. Solar technology recommendations for the critical area in feasibility study I.

Glass-to-glass solar cells are recommended for the windows. Based on these technologies, and consider that the buildings have residential functions, the solar energy produced from PV systems can cover up to 15% of the energy needs of the buildings in the critical area.

In the feasibility study II, the critical area (27,350 m^2) chosen for detailed analysis is characterized by the presence of various building typologies, such as the high-rise buildings, which affect the surrounding buildings with significant overshadowing throughout the year.

The area consists of six mixed-use structures (service and residential buildings), where 54% of the total solar irradiation is caused by diffuse irradiation and inter-buildings reflections, while 46% is from direct irradiation. The direct irradiation on the roofs accounts for 47% or the total irradiation, while 53% is from the combination of diffuse irradiation and solar reflections from the surrounding ground. In the case of façades, 85% of total irradiation is from diffuse irradiation and solar inter-building reflections, while 15% is from direct irradiation (Figure 24).

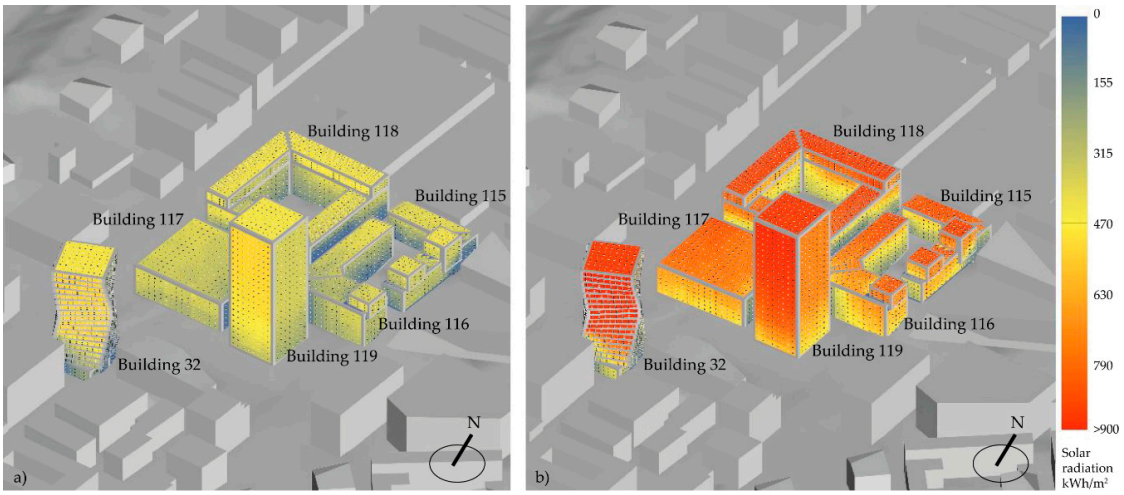

Figure 24. Analysis of direct solar irradiation (**a**) and global solar irradiation analysis (**b**) in the critical area for feasibility study II.

The solar analysis shows that for the high-rise buildings, Building 32 and Building 119 (Figure 24), the direct solar irradiation is almost double the irradiation on the roof.

However, because of the presence of the towers, the façades and the roofs of the nearby buildings have a significant reduction of solar energy potential (Figure 25). Regarding the energy generation (Figure 26), the towers' roofs (no. 9 of Building 119 and no. 0 of Building 32) show the highest solar potential, while for façades these are the ones oriented southeast on the two towers (no. 2 and no. 3 in Building 32 and no. 5 and no. 6 in Building 119).

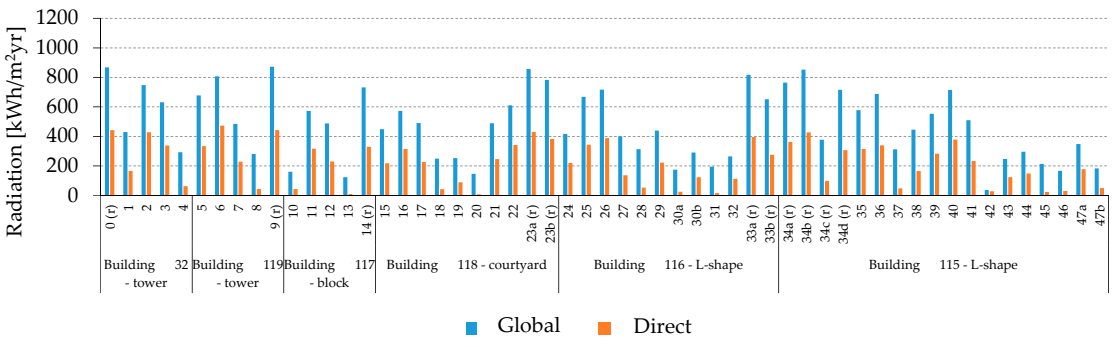

Figure 25. Average irradiation on the roofs (r) and façades in the critical area for feasibility study II.

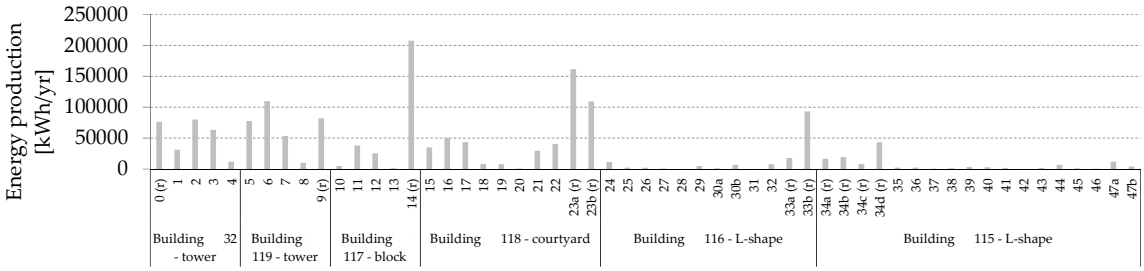

Figure 26. Solar energy generation on roofs (r) and façades in the critical area for feasibility study II.

However, for those buildings, because of the high energy demand of such buildings, the energy generated from the solar systems only covers 8% and 12% of the energy needs for Building 119 and Building 32, respectively. Regarding the office buildings, the potential is the highest for Building 117, for which the solar energy covers 44% of its total energy needs (Table 13).

Table 13. Energy coverage potential by solar technologies in the critical area for feasibility study II.

Building Type	Building No.	BRA (m^2)	Total Energy Needs (kWh/year)	Solar Irradiation Potential Coverage—Façades and Roofs (kWh/year)	Solar Energy Potential Coverage—Windows (kWh/year)	Energy Coverage Estimation by PV
Office	32—tower	27,000	2,430,000	262,038	39,468	12%
	119—tower	52,900	4,761,000	332,219	53,143	8%
	117—block	7215	649,350	276,562	11,967	44%
Residential	118—courtyard	37,307	3,171,095	484,735	20,150	16%
	116—L-shape	16,034	1,362,890	146,989	6199	11%
	115—L-shape	11,810	1,003,808	138,636	4927	14%

The solar energy generation from PV systems installed on the building envelope in courtyard Building 118 can cover 16% of its energy demands, while in the L-shaped Building 115 and Building 116 it can cover 11% and 14% of their energy needs, respectively (Table 13).

The solar energy calculation considers the reduction factor, which is 75% for all of the roofs, while for the façades, the reduction factors are 47% and 52% for high-rise buildings and mid-rise office buildings, respectively. In the case of the façades of residential buildings, the reduction factor is 46% for courtyard structures and 22% for L-shaped dwellings. Regarding the technology recommendations (Figure 27), the highly efficient monocrystalline BAPV system can be installed on flat roofs, while glass–glass or thin film PV systems are suited for transparent surfaces and façades.

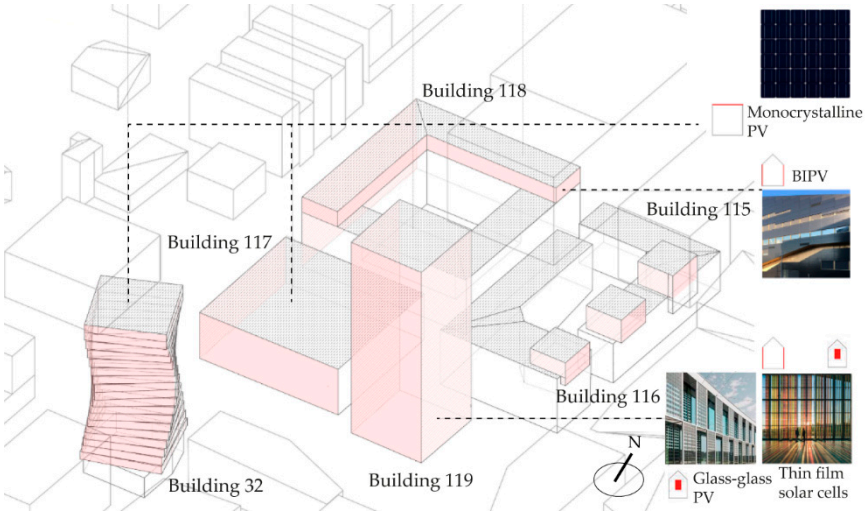

Figure 27. Solar technology recommendations for the critical area for feasibility study II.

5. Discussion

The increase of the supply energy from decentralized RES (by reducing the energy demand of the building stock) requires new applicable methodologies to integrate useful data into the energy mapping systems in order to effectively support the real building process by promoting decision making and real actions. The available surfaces of the built environment are very promising sources for solar system integration. As such, the exploitation of their potential is a priority strategy towards their implementation in energy-efficient neighborhoods. A multidisciplinary approach is essential to include the building aspects within the real potential estimation of the built environments.

In this framework, this study aims to propose an approach to cover the existing research gaps on the definition of urban solar maps. Previous studies have demonstrated that Daysim, a Radiance-based software used for the solar analysis in this approach, accurately calculates solar irradiation in complex urban environments [7,16,28,41] by considering the overshadowing effect from other buildings and solar inter-building and ground reflections. This allows evaluation of solar energy potential at the neighborhood scale by showing the potential of roofs and façades, which are not actually available in most of the existing solar maps. Furthermore, this also means that 3D solar maps can visualize solar potential of the whole neighborhood's surfaces and show solar availability in connection to the relevant urban indicators, such as urban density, morphology, H/W, and BRA.

Another novelty of this approach is the application of reduction factors of solar potential that consider the analysis of local building typological aspects. Their application allows a more accurate estimation of solar potential depending on building typologies, architectural features, and construction constraints. In the analyzed scenarios, 22–53% of façade surfaces are suitable for solar system installation. When residential buildings are considered, the available area is smallest in the case of L-shaped buildings, where on average only 22% of the façade area can be considered because of the presence of: (i) transparent surfaces (windows) to guarantee indoor daylight visual comfort and solar gain penetration, (ii) obstructions (e.g., balconies, external staircases), and (iii) self-shading. Despite those constraints, for U-shaped buildings and row houses, more than 45% of façades are suited for PV system installation, while for linear residential buildings, more than 50% of the available area is suitable for PV installation on the façades. In the case of office buildings characterized by simpler and more linear forms as well as the low presence of architectural features and construction constraints (e.g., no balconies or self-shading elements), the usable area is more than 50%. Here, the most important reduction factor influencing the solar potential is the presence of windows. Finally, a detailed irradiation analysis in selected critical areas allows identification of the best solar technologies suited to local conditions, such as exposure to direct or diffuse and reflected irradiation, shading, and orientation of the building envelope elements. Solar technologies available on the market today are not limited to PV systems on roofs, rather there are numerous technologies that can be integrated into the façades, windows, and balconies, with increasingly innovative and customizable solutions. In that regard, the solar energy generation analysis conducted in the critical areas shows that solar systems can cover between 8% and 44% of the total energy needs of the buildings, depending on the urban morphology and adopted technology.

Limitations of the Study

There are several limitations associated with the developed approach.

Firstly, when making solar maps at the district scale, average values of solar irradiation for a point in the middle of the façades and roofs are considered. However, the solar potential can vary significantly on the surfaces of the building's envelope because of the self-shading by other parts of the building, presence of the surrounding buildings, etc. Therefore, a more refined grid-based analysis, such as the example performed in Step 6 of the critical areas, should be conducted at the district scale. In terms of shading, the vegetation elements are not considered. In this case, LiDAR technology can overcome this gap by building a more detailed 3D model with locations and presence of trees. LiDAR technology can also be used to build a more refined 3D model of the buildings by detailing all of the architectural

features (obstructions, windows, etc.) on the roofs and on the façades, avoiding the application of the reduction factors.

Secondly, PV energy production calculation is based on a simplified equation that provides an estimation of the PV energy generation without considering typical system design aspects (i.e., the losses caused by the local shading on module strings, the energy conversion from solar energy to electric energy, and transportation losses from the surface of the panel to the system for energy conversion). This gap can be covered, for example, by using dedicated software for more accurate solar energy production calculations when the specific photovoltaic system is designed. Further studies are also required for seasonal variations in solar energy production.

Thirdly, the research scope is limited to solar PV systems, given that electrical energy is the main supply system in Norway. However, the approach can also be used for other systems, such as ST installations. Furthermore, financial aspects and payback time connected to PV systems were not considered in this study.

Another limitation is associated with aesthetic evaluation of solar systems at the district scale. The aesthetic evaluation of integration of solar energy systems can be assessed by using tools such as LESO-QSV [42].

Lastly, the values of reduction indicators due to transparent surfaces, architectural obstructions, and self-shading of the building are based on analysis of local building features in Trondheim; therefore, their definition and solar potential can vary substantially depending on the building typology, local architectural features, and climate conditions.

6. Conclusions and Outlook to Further Work

This study presents a methodological approach to estimate the solar energy potential at the neighborhood scale, considering local shadowing and inter-building effects, as well as the analysis of local building typological aspects. By analyzing urban parameters and creating solar maps of the built areas, a relation between building typologies, urban and building factors (e.g., orientation of the façades and roofs, morphology, H/W, height of the structures), and solar energy potential was studied. The outcomes confirmed that no façade orientation was identified as the optimal one [28]. Regarding building design and solar energy generation potential, the following outcomes specific to the latitude of Trondheim can be confirmed:

- High-rise buildings have a high potential for BIPV façade integration, even though in the analyzed scenario the energy coverage by solar systems is quite low. Solar systems for buildings higher than 40 m can cover only up to 12% of the total energy needs.
- High-rise buildings produce significant shading in all seasons (even in the summer, when the sun angle is as high as 60° at Trondheim's latitude) on the surrounding buildings. High-rise buildings reduce the solar potential of the surrounding buildings by lowering solar energy production potential by 15%. This latter percentage strictly depends on the local urban scenario.
- Low-rise buildings characterized by lower energy demand, such as linear buildings, row houses, and simple blocks with considerable roof area (flat or pitched), are the most suitable building typologies for rooftop PV system installation, with potential energy coverage by solar systems ranging from 26% to 44% depending on the local conditions.
- L-shaped and U-shaped buildings are characterized by low suitability for solar system installation due to shadowing from the surrounding buildings. For those buildings, the energy generation from solar systems can cover up to 11%–14% and 16% of their total energy needs, respectively.

Furthermore, the application of reduction factors related to architectural and geometrical building features allowed estimation of solar potential by considering transparent surfaces and obstructions, while detailed irradiation analysis allowed the best locations with high solar potential to be identified and the most suitable PV technologies to be chosen based on the local conditions.

Some of the major advantages of the developed approach are its applications, as follows. The approach can:

- Provide a support planning decision-making instrument to consider the solar energy integration since in early design stages by identifying the most suitable building surfaces, roofs, and façades for BIPV installations in both new and consolidated urban areas.
- Evaluate and compare the solar potential of different project scenarios.
- Optimize the solar energy potential of projects currently under development by controlling their impact on the solar accessibility of the existing buildings.

Several target groups can use this approach to assess solar energy potential at the district scale, such as:

1. Architects. There is a false myth that among architecture professionals, the implementation of solar energy technologies on buildings compromises their aesthetics and proportions [43]. Solar technologies available today show that there are many ways to integrate solar energy technologies into a building's exterior, and installing building-added PV systems on roofs is not the only or most effective solution in many cases.
2. Urban planners. Urban planners focus their work on designing public spaces, regulating land use in the projects of existing and new neighborhoods. Often solar energy is not a priority, and urban planners do not always have competences to evaluate the design based on the energy performance of PV systems [44]. This study shows how solar potential evaluation can be implemented in the design process.
3. City authorities. This methodology can be used as an energy-planning instrument by urban decision makers by localizing the most suitable urban surfaces for solar energy system integration.
4. Citizens. Solar maps developed at the city scale can be used as informative tools to showing the buildings' owners the potential for solar energy generation on the building envelope.

Finally, the application of this approach in different building and urban scenarios (i.e., the existing situation and the two feasibility studies) showed that it can be used independently for several design proposals. Furthermore, the tools used to develop this approach are popular among architects and urban planners, therefore it can be used by anyone with suitable software skills. The climate data used in this study (through the weather climate file (.epw)) can be substituted with any other worldwide location, and therefore, it can be replicated in any city. The building archetypes that define the reduction factors can be also replaced by building typologies unique to any location. For the further development of the proposed approach, several aspects could be considered:

1. Evaluation of Life-Cycle Assessment and energy saving in terms of reduction of GHG emissions. Energy generated by solar systems contributes to reducing carbon and energy footprints in built environments [45].
2. Potential of ST energy and ST system integration.
3. Accessibility of sunlight at the ground level to design more attractive outdoor urban areas.
4. Microgrid and storage solutions for solar energy at the neighborhood scale.
5. Analysis to maximize the solar potential of a building, ensuring good indoor daylight conditions.
6. Develop 3D model applications to visualize and quantify energy production, along with environmental and economic impacts of the PV integration.
7. Further studies are required on the influence of solar inter-building and ground reflections on the solar potential and reduction factors. An earlier study conducted for the Øvre Rotvoll neighborhood in Trondheim showed that different finishing materials used on the façades of the buildings and terrain had a significant influence on the solar reflections, which can compensate for losses due to shadowing caused by the surrounding buildings. The presence of snow in combination with light-colored façade finishing materials can improve the solar availability by around 20% [28].

Author Contributions: Conceptualization, G.L., M.M.L., E.S. and P.B.; data curation, G.L. and M.M.L.; formal analysis, G.L., M.M.L. and E.S.; investigation, G.L., M.M.L. and E.S.; methodology, G.L., M.M.L., E.S., P.B. and F.F.; software, M.M.L., E.S., P.B. and F.F.; supervision, G.L., P.B. and F.F.; validation, E.S.; visualization, M.M.L.; Writing—Original draft, G.L.; Writing—Review and editing, M.M.L., E.S., P.B. and F.F.

Funding: The APC was funded by Norwegian University of Science and Technology.

Acknowledgments: The authors wish to thank Emerita Anne Grete Hestnes for her advice and shared experience during the development of this research work, and Luca Finocchiaro and Inger Andersen for their feedback during the advancement of the work. Furthermore, the authors wish to thank Erik Stenman and Adnan Harambasic for sharing materials needed for the development of the 3D model to conduct the analyses in the feasibility studies. This article is based upon work from European Cooperation in Science and Technology (COST) Action CA16235 PEARL PV, supported by COST.

Conflicts of Interest: The authors declare no conflict of interest.

References

1. Amado, M.; Poggi, F. Solar Energy Integration in Urban Planning: GUUD Model. *Energy Procedia* **2014**, *50*, 277–284. [CrossRef]
2. Beckers, B. *Solar Energy at Urban Scale*; Wiley-ISTE: New York, NY, USA, 2012.
3. United Nations, Department of Economic and Social Affairs, Population Division. *World Population Prospects: The 2015 Revision, Key Findings and Advance Tables*; United Nations: New York, NY, USA, 2015.
4. Kabir, E.; Kumar, P.; Kumar, S.; Adelodun, A.A.; Kim, K. Solar energy: Potential and future prospects. *Renew. Sustain. Energy Rev.* **2018**, *82*, 894–900. [CrossRef]
5. Lobaccaro, G.; Croce, S.; Lindkvist, C.; Munari Probst, M.; Scognamiglio, A.; Dahlberg, J.L.M.; Wall, M. A cross-country perspective on solar energy in urban planning: Lessons learned from international case studies. *Renew. Sustain. Energy Rev.* **2019**, *108*, 209–237. [CrossRef]
6. Bonomo, P.; Polo López, C.S.; Saretta, E.; Corti, P.; Frontini, F. bFAST: A Methodology for Assessing the Solar Potential of Façades in Existing Building Stocks. In Proceedings of the Conference: ISES EuroSun 2018 Conference—12th International Conference on Solar Energy for Buildings and Industry, Rapperswil, Switzerland, 10–13 September 2018.
7. Good, C.S.; Lobaccaro, G.; Hårklau, S. Optimization of Solar Energy Potential for Buildings in Urban Areas —A Norwegian Case Study. *Energy Procedia* **2014**, *58*, 166–171. [CrossRef]
8. Hestnes, A.G. Building integration of solar energy systems. *Sol. Energy* **1999**, *67*, 181–187. [CrossRef]
9. Desthieux, G.; Carneiro, C.; Camponovo, R.; Ineichen, P.; Morello, E.; Boulmier, A.; Abdennadher, N.; Dervey, S.; Ellert, C. Solar Energy Potential Assessment on Rooftops and Façades in Large Built Environments Based on LiDAR Data, Image Processing, and Cloud Computing. Methodological Background, Application, and Validation in Geneva (Solar Cadaster). *Front. Built Environ.* **2018**, *4*, 14. [CrossRef]
10. Desthieux, G.; Carneiro, C.; Susini, A.; Abdennadher, N.; Boulmier, A.; Dubois, A.; Camponovo, R.; Beni, D.; Bach, M.; Leverington, P.; et al. Solar cadaster of Geneva: A decision support system for sustainable energy management. In *From Science to Society*; Otjacques, B., Hitzelberger, P., Naumann, S., Wohlgemuth, V., Eds.; Springer: Cham, Switzerland, 2018; pp. 129–137.
11. Redweik, P.; Catita, C.; Brito, M. Solar energy potential on roofs and façades in an urban landscape. *Sol. Energy* **2013**, *97*, 332–341. [CrossRef]
12. Saretta, E.; Bonomo, P.; Frontini, F. A Calculation Method for the BIPV Potential of Swiss Façades at LOD2.5 in Urban Areas: A Case from Ticino Region. *Sol. Energy* **2019**, submitted.
13. IEA SHC Task 51 Solar Energy in Urban Planning. In *Approaches, Methods and Tools for Solar Energy in Urban Planning*; International Energy Agency: Paris, France, 2018.
14. Kanters, J.; Wall, M.; Kjellsson, E. The solar map as a knowledge base for solar energy use. *Energy Procedia* **2014**, *48*, 1597–1606. [CrossRef]
15. Lobaccaro, G.; Frontini, F.; Masera, G.; Poli, T. SolarPW: A new solar design tool to exploit solar potential in existing urban areas. *Energy Procedia* **2012**, *30*, 1173–1183. [CrossRef]
16. Jakubiec, J.; Reinhart, C. A method for predicting city-wide electricity gains from photovoltaic panels based on LiDAR and GIS data combined with hourly Daysim simulations. *Sol. Energy* **2013**, *93*, 127–143. [CrossRef]
17. Freitas, S.; Catita, C.; Redweik, P.; Brito, M. Modelling solar potential in the urban environment: State-of-the-art review. *Renew. Sustain. Energy Rev.* **2015**, *41*, 915–931. [CrossRef]

18. Solcellespesialisten. *Solar Map of Norway*; Solcellespesialisten: Fredrikstad, Norway, 2019.
19. Swiss Federal Office of Energy SFOE. Federal Office of Meteorology and Climatology MeteoSwiss. Federal Office of Topography swisstopo, Solar Map of Switzerland. Available online: https://www.uvek-gis.admin.ch/BFE/sonnenfassade/index.html?lang=en (accessed on 8 August 2019).
20. Klauser, D. *Suitability of Roofs for Use of Solar Energy/Solarpotentialanalyse Für Sonnendach.ch. Schlussbericht*; Meteotest for Swiss Federal Office of Energy: Bern, Switzerland, 2016.
21. Meteorologisk Institutt. Værvarsel for Trondheim. 2018. Available online: https://www.yr.no/sted/Norge/Tr%C3%B8ndelag/Trondheim/Trondheim/ (accessed on 8 August 2019).
22. Nilsen, J. Ville kle Bygget Med Grønne Solceller—Endte Opp Med Helt ny Teknologi. 2015. Available online: https://www.tu.no/artikler/ville-kle-bygget-med-gronne-solceller-endte-opp-med-helt-ny-teknologi/275882 (accessed on 8 August 2019).
23. Solenergi FUSen. Referanseprosjekter fra Solenergi FUSen. 2019. Available online: https://www.fusen.no/prosjekter (accessed on 8 August 2019).
24. Johanessen, T. Verdens Nordligste Plusshus Åpner Dørene. 2019. Available online: https://www.tu.no/artikler/verdens-nordligste-plusshus-apner-dorene/458951 (accessed on 8 August 2019).
25. Hegli, T. Presentasjon av Skisser. Powerhouse-Alliansens to Første Prosjekter. 2012. Available online: http://www.zeb.no/index.php/en/conference/item/413-presentasjon-av-skisser-powerhouse-alliansens-to-f%C3%B8rste-prosjekter (accessed on 8 August 2019).
26. Fufa, S.; Andresen, I.; Schlanbusch, R.D.; Kjendseth Wiik, M.; Sørnes, K. *A Norwegian ZEB Definition Guideline*; SINTEF Academic Press: Oslo, Norway, 2016.
27. Multiconsult and Asplan Viak. *Solcellesystemer Og Sol i Systemet*; Solenergiklyngen: Kjeller, Norway, 2018.
28. Lobaccaro, G.; Carlucci, S.; Croce, S.; Paparella, R.; Finocchiaro, L. Boosting solar accessibility and potential of urban districts in the Nordic climate: A case study in Trondheim. *Sol. Energy* **2017**, *149*, 347–369. [CrossRef]
29. Jones, A.D.; Underwood, C.P. A thermal model for photovoltaic systems. *Sol. Energy* **2001**, *70*, 349–359. [CrossRef]
30. Miljøverndepartementet. Nasjonale Forventninger til Regional og Kommunal Planlegging. Available online: https://www.regjeringen.no/no/dokumenter/nasjonale-forventninger-til-regional-og-/id649919/ (accessed on 8 August 2019).
31. Trondheim Kommune. *Kommunedelplan: Energi og Klima 2017–2030*; Trondheim Kommune: Trondheim, Norway, 2017.
32. FME Zero Emission Neighborhoods in Smart Cities. ZEN Pilot Projects. Available online: https://fmezen.no/knowledge-axis-trondheim/ (accessed on 8 August 2019).
33. Trondheim Kommune. Kommunedelplan for Sluppen—Mulighetsstudie Sluppen 2050. Available online: https://sites.google.com/trondheim.kommune.no/kdpsluppen/mulighetsstudiet-sluppen-2050 (accessed on 8 August 2019).
34. Direktoriat for Byggkvalitet. Byggteknisk Forskrift (TEK17). 2017. Available online: https://www.regjeringen.no/contentassets/20503ddfe0664fac9e2185c1a6c80716/veiledning-til-byggteknisk-forskrift-tek17_01_07_2017_oppdatert_15_09_2017.pdf (accessed on 8 August 2019).
35. Fath, K.; Kuhn, T.E.; Schultmann, F.; Sprenger, W.; Stengel, J. A method for predicting the economic potential of (building-integrated) photovoltaics in urban areas based on hourly Radiance simulations. *Sol. Energy* **2015**, *116*, 357–370. [CrossRef]
36. Kanters, J.; Horvat, M. Solar energy as a design parameter in urban planning. *Energy Procedia* **2012**, *30*, 1143–1152. [CrossRef]
37. IEA SHC Task 41 Solar Energy and Architecture. T.41.A.2: Solar Energy Systems in Architecture—Integration Criteria and Guidelines. 2013. Available online: http://task41.iea-shc.org/Data/Sites/1/publications/T41DA2-Solar-Energy-Systems-in-Architecture-28March2013.pdf (accessed on 8 August 2019).
38. Saretta, E.; Bonomo, P.; Frontini, F. Active BIPV Glass Façades: Current Trends of Innovation. In Proceedings of the Glass Performance Days 2017, Tampere, Finland, 28–30 June 2017.
39. EPFL—École Polytechnique Fédérale de Lausanne. EPFL's Campus has the World's First Solar Window. Available online: https://actu.epfl.ch/news/epfl-s-campus-has-the-world-s-first-solar-window/ (accessed on 8 August 2019).
40. Krippner, R. *Building-Integrated Solar Technology: Architectural Design with Photovoltaics and Solar Thermal Energy*; DETAIL: München, Germany, 2017.

41. Lobaccaro, G.; Croce, S.; Vettorato, D.; Carlucci, S. A holistic approach to assess the exploitation of renewable energy sources for design interventions in the early design phases. *Energy Build.* **2018**, *175*, 235–256. [CrossRef]
42. Probst, M.C.M.; Roecker, C. Criteria and policies to master the visual impact of solar systems in urban environments: The LESO-QSV method. *Sol. Energy* **2019**, *184*, 672–687. [CrossRef]
43. Dunay, R.; Schubert, R.; Wheeler, J. No Compromise: The Integration of Technology and Aesthetics. *J. Archit. Educ.* **2016**, *60*, 8–17. [CrossRef]
44. Kanters, J.; Wall, M. Experiences from the urban planning process of a solar neighbourhood in Malmö, Sweden. *UrbanPlan. Transp. Res.* **2018**, *6*, 54–80. [CrossRef]
45. Tiantian, Z.; Meng, W.; Hongxing, Y. A Review of the Energy Performance and Life-Cycle Assessment of Building-Integrated Photovoltaic (BIPV) System. *Energies* **2018**, *11*, 3157.